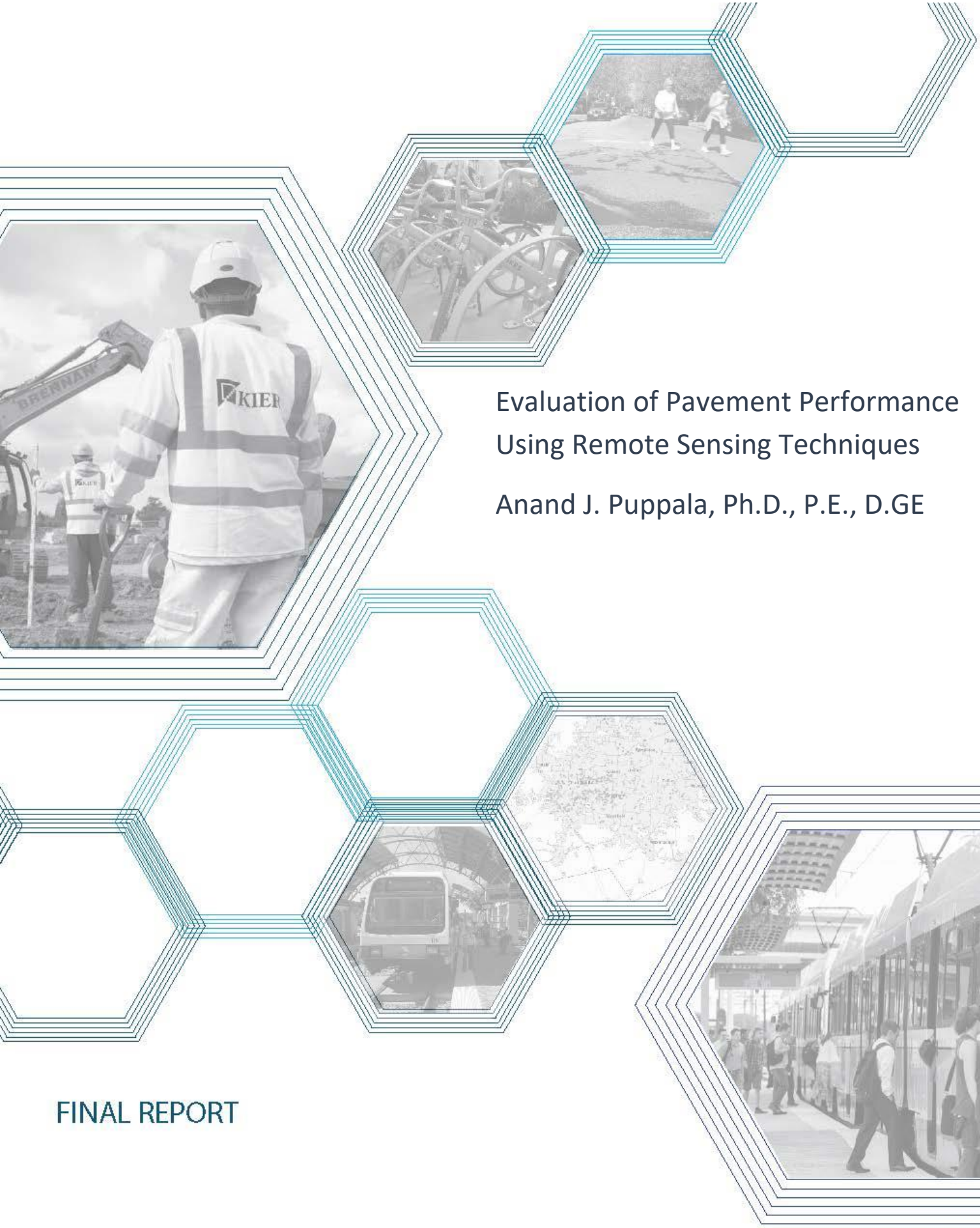

Evaluation of Pavement Performance Using Remote Sensing Techniques

Anand J. Puppala, Ph.D., P.E., D.GE

FINAL REPORT

CTEDD
Center for Transportation Equity, Decisions & Dollars

EVALUATION OF PAVEMENT PERFORMANCE USING REMOTE SENSING TECHNIQUES

FINAL PROJECT REPORT

by

Anand J. Puppala, Ph.D., P.E., D.GE
The University of Texas at Arlington

Sponsored by CTEDD

for
Center for Transportation, Equity, Decisions and Dollars **(CTEDD)**
USDOT University Transportation Center
The University of Texas at Arlington
601 W.Nedderman Dr. Suite 103
Arlington TX 76019-0108 United States
Phone: 817-272-5138 | Email: C-Tedd@uta.edu

In cooperation with US Department of Transportation-Research and Innovative Technology Administration (RITA)

Acknowledgment

This work was supported by a grant from the Center for Transportation Equity, Decisions and Dollars (CTEDD) funded by U.S. Department of Transportation Research and Innovative Technology Administration (OST-R) and housed at The University of Texas at Arlington.

Disclaimer

The contents of this report reflect the views of the authors, who are responsible for the facts and the accuracy of the information presented herein. This document is disseminated under the sponsorship of the U.S. Department of Transportation's University Transportation Centers Program, in the interest of information exchange. The Center for Transportation, Equity, Decisions and Dollars (CTEDD), the U.S. Government and matching sponsor assume no liability for the contents or use thereof

Technical Report Documentation Page

1. Report No.	2. Government Accession No.	3. Recipient's Catalog No.
CTEDD: 017-10		

4. Title and Subtitle	5. Report Date
Evaluation of Pavement Performance Using Remote Sensing Techniques	Feb 22, 2019
	6. Performing Organization Code

7. Author(s)	8. Performing Organization Report No.
Anand J. Puppala, Ph.D., P.E., D.GE Surya S. C. Congress, Ph.D.	

9. Performing Organization Name and Address	10. Work Unit No. (TRAIS)
Center for Transportation, Equity, Decisions and Dollars (CTEDD) USDOT University Transportation Center The University of Texas at Arlington 601 W.Nedderman Dr. Suite 103 Arlington TX 76019-0108 United States	11. Contract or Grant No.

12. Sponsoring Organization Name and Address	13. Type of Report and Period Covered
United States of America Department of Transportation Research and Innovative Technology Administration	14. Sponsoring Agency Code

15. Supplementary Notes

Report uploaded at www.ctedd.uta.edu

16. Abstract

Infrastructure monitoring often requires interaction between the data collector and the traffic which leads to traffic delays as well as exposing the personnel to perilous conditions. Of late, different sensors like Light Detection and Ranging (LiDAR) and visible range cameras mounted on various platforms classified as terrestrial and aerial have been used to remotely inspect the infrastructure assets. Due to the advancement of these sensors, application of remote sensing techniques for monitoring infrastructure has gained lot of impetus in the past decade. The proposed research focused on monitoring the transportation infrastructure using terrestrial LiDAR and unmanned aerial vehicle-close range photogrammetry (UAV-CRP) technologies. The condition of the pavement infrastructure assets located in Dallas-Fort worth areas were monitored using these technologies. The soils in this area undergo swell-shrink behavior, causing premature failure of pavements resulting in several millions of dollars of expenditures annually for their rehabilitation works. The adopted procedures for the monitoring techniques and solutions can immediately benefit transportation agencies to easily obtain the valuable information in a safe manner.

17. Key Words	18. Distribution Statement
	No restrictions.

19. Security Classification (of this report)	20. Security Classification (of this page)	21. No. of Pages	22. Price
Unclassified.	Unclassified.	38	NA

Table of Contents

Table of Figures

1 INTRODUCTION

In the USA, bump is one of the prevalent problems experienced at the approach of bridge structure. Annually, millions of dollars are spent by state transportation agencies to repair this bump issue. Differential settlement of backfill materials and foundation soils, as well as the erosion of backfill are identified as major contributing factors (Anand J. Puppala et al., 2018). The State of Texas predominantly experiences pavement failures at sites with high sulfate concentration in soils (8000 ppm or higher). Many of those failures could be attributed to sulfate-induced soil heave caused due to the formation of an expansive mineral called Ettringite (Puppala et al., 2012). It is formed from the calcium-based stabilizers reacting with water, clay, and sulfates in the soil. The current stabilization practices for high sulfate soils need high maintenance costs and pose safety concerns due to the distress that these pavements undergo. Many districts have to partially or completely rehabilitate these pavements built on high sulfate soils within a few years from original construction/rehabilitation. Most of those repairs include a complete reclamation of the pavement lanes for several miles, which incur higher expenditures.

Human-made lightweight backfill materials are being used to mitigate the bump issues at the bridge approach. Increasing the mellowing time to prevent the formation of ettringite have shown good results in arresting the heave in pavements laid over sulfate soils (Puppala et al., 2005). However, the effectiveness of using the above discussed treatments need to be validated using field monitoring data. Traditional methods result in higher inspection costs and traffic delays. In this research, two sites were selected and monitored using remotely sensing equipment. These techniques not only help in reducing the inspection costs but also in cutting down the traffic delay costs incurred during traditional pavement inspection methods. Second section deals with the site details and third section discusses about the testing methods available in the literature. Fourth section covers the laboratory testing of soil samples collected at the two sites. Fifth section comprises of the field studies conducted using cutting-edge technologies. The last section summarizes and concludes about the research findings.

2 BACKGROUND

2.1 Site Details

2.1.1 Bridge Approach Site

Texas Department of Transportation, Fort Worth District (TxDOT-FTW) has implemented a new material, Expanded Polystyrene (EPS) geofoam, in rehabilitation of an adjacent embankment of the 40-ft. high bridge located on US 67 over SH 174 in Johnson County, Cleburne, Texas. The top 6 ft. of the existing embankment fill soil had been replaced by approximately 35,000 ft^3 of EPS 22 geofoam blocks. As a result, loads imposed on the underlying subgrade have reduced. Consequently, magnitude of settlement due to the consolidation of foundation material could be controlled. The objective of this research study is to determine the performance of lightweight backfill, in the form of EPS geofoam, to mitigate embankment settlements.

During the rehabilitation of the embankment, four casings of diameter 3.3 inch (8.5 cm) and length 22 ft (6.7 m) each were fixed on top of EPS 22 geofoam layer in the test embankment which is at a depth of about 2 ft (0.6 m) below the pavement surface. Beginning at the far end of the casing, the probe is driven into the casing through a connected pipe and readings are recorded after every two feet with the readout device called "Digitilt DataMate" (Ruttanaporamakul, 2015). The profile of the casing can be measured by plotting the measurements. Any deviation in the profile of the casing compared to the initial profile from subsequent surveys indicate movement of the casing caused due to the movement of the supporting surface. The vertical displacements had been recorded cumulatively from the initial readings collected at the time of installation. The drawback of this method is that it only provides the movements near to the casing locations.

2.1.2 Pavement Heaving Site

Pavement constructed on US SH 82 near Paris district, Texas experienced heaving due to the presence of high sulfates in the soils. The formation of Ettringite and crystal growth have been identified as significant contributors of soil swelling. Swell behavior of the treated soils at respective mellowing periods could be attributed to the variation in the amounts of sulfates, reactive alumina, and silica contents. The soils treated with lime are subjected to extended periods of mellowing to arrest the formation of Ettringite. Soils treated with higher mellowing periods exhibited lesser sulfate induced heaving when the concentration of sulfate is less than 30,000 ppm. At higher sulfate levels, the

mellowing did not result in effective treatment of soils. The test sections laid over the treated soils need to be monitored to validate the effectiveness of the treatments. Remote sensing data collection methods are used and the details are discussed in the following sections.

3 LITERATURE REVIEW

3.1 Testing methods

Some of the current practices for assessment of pavement performance and pavement condition include Falling Weight Deflectometer (FWD), Light Falling Weight Deflectometer (LFWD), and Plate Load Tests (PLT) and profilometer surveys. Falling weight deflectometers (FWDs) have been used to evaluate the condition of pavements since the 1980s, shown in Figure 1a. The pavement deflections are measured in response to a stationary dynamic load, simulating the passing wheel load. Using this data, structural capacity of pavements is evaluated for pavement maintenance purposes (Alavi et al., 2008). LFWD is a compact equipment that can be used for determining the dynamic modulus of the inspecting layer, shown in Figure 1b. Depending upon the manufacturers and countries of origin, several variants of LFWD with similar working principle are available in the market. LFWD generally comprises of equipment that generates a defined load pulse, a loading plate, and geophone sensors to measure the reaction of the center of the plate. The load pulse and deflection are used to back-calculate the layer properties (Alshibli et al., 2005).

(a)

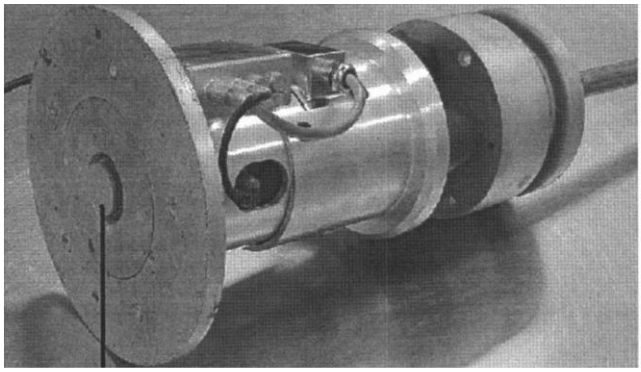

(b)

Figure 1. Testing Methods used for Pavement Evaluation (a) Falling Weight Deflectometer (FWD) (b) Light Falling Weight Deflectometer (LFWD) (Alshibli et al., 2005)

Plate Load Test (PLT) has been used to evaluate the strength/stiffness of pavement layers composed of different materials. In this tests, a static load is applied through a hydraulic jack with regular increments on a 30 cm diameter plate placed on top of the pavement layer that needs to be evaluated. Deformation response for each load increment is measured and used to produce a load deflection curve (Alshibli et al., 2005). Profiler measures the true profile along the path it traverses on the pavement. The profile data is used to calculate two important parameters "Present Serviceability Index –PSI" and "International Roughness Index – IRI" that help in analyzing the condition of the pavement. All these methods discussed above are either costly or laborious. Hence, the present research study identified the need for using remotely sensing data collection methods that can collect the data without interacting with the traffic.

3.2 Sampling Rate

Current standards and specifications for testing and the sampling rate in the field also vary among different state agencies as shown in Table 1. It should be noted that the specifications for each state agency provided in Table 1 are only a representative portion of the entire specification.

Table 1. Specifications for testing and the sampling rate in the field

Agency	Specifications	Reference Manual
Texas DOT (TxDOT)	Untreated Base Courses: 1 minimum test result per 3,000 C.Y per lift for in-place density	TxDOT: Guide Schedule of Sampling & Testing
	Treated Subgrade and Base Courses: 1 minimum test result per 3,000 C.Y per lift for in-place density	
North Dakota (NDDOT)	1 test result per 5,000 S.Y. rural or 1500 S.Y. urban of concrete pavement for materials finer than No. 200 sieve	Section 500: Rigid Pavement
	1 test result per 5,000 S.Y. rural or 1500 S.Y. urban of concrete pavement for fine and coarse aggregates	
Arizona DOT (ADOT)	Proctor Density and Optimum Moisture: one per soil type, and as needed	Section 203: Materials Quality
	Compaction and Gradation: one per 1500 ft. or change in material	

		Assurance Program
Colorado DOT (CDOT)	1 test per 2000 cu yds. or fraction thereof of testable material as described in CDOT standard specifications	Section 203: Materials Quality Assurance program
	Density: 1 per 500 cu yds. when within 100 ft. of bridge approach	
Virginia DOT (VDOT)	1 test per 4 roadway miles, or fraction thereof, consisting of the average of 5 readings. Minimum of 5 readings per project, unless total quantity of individual material is less than 500 tons per project	Section 206: Methods and Frequencies of Sampling

From Table 1, it can be observed that different agencies follow different sampling rate due to various reasons. This results in an subjective assessment of the pavement condition. This research also focuses on transforming present subjective evaluation of pavement to more objective and reliable manner.

3.3 Cutting-edge Technologies for Performance Monitoring of Pavement

The advent of contactless data collection procedures and equipment has provided a solution to obtain detailed pavement condition data with minimum traffic interaction. Terrestrial Light Detection and Ranging (LIDAR) and unmanned aerial vehicles coupled with photogrammetry are the two technologies used in this study for monitoring the pavement health. Due to the non-intrusive nature of data collection they provide the surficial condition of the pavement without obstructing the traffic.

3.3.1 Light Detection and Ranging (LiDAR)

Light Detection and Ranging (LIDAR) is used to map the area by emitting laser pulses on to the surroundings and receiving them. FARO FOCUS series X 330 Laser Scanner, as shown in Figure 2a, is utilized in this research to perform LIDAR investigations. X330 has a scanning range of 330 m and is equipped with GPS and remote scanning features. SCENE 5.4 software is used for registering and post processing the image files for construction of 3D cloud space of the scanned area. Constructed cloud space and associated data set are then transferred to builder application for further analysis. From Figure 2a, it can be observed that the first step for performing the LiDAR

surveys is to schedule a scanning plan. This includes determining how many scans must be performed at the test site, resolution of the scans and placement of the LiDAR equipment.

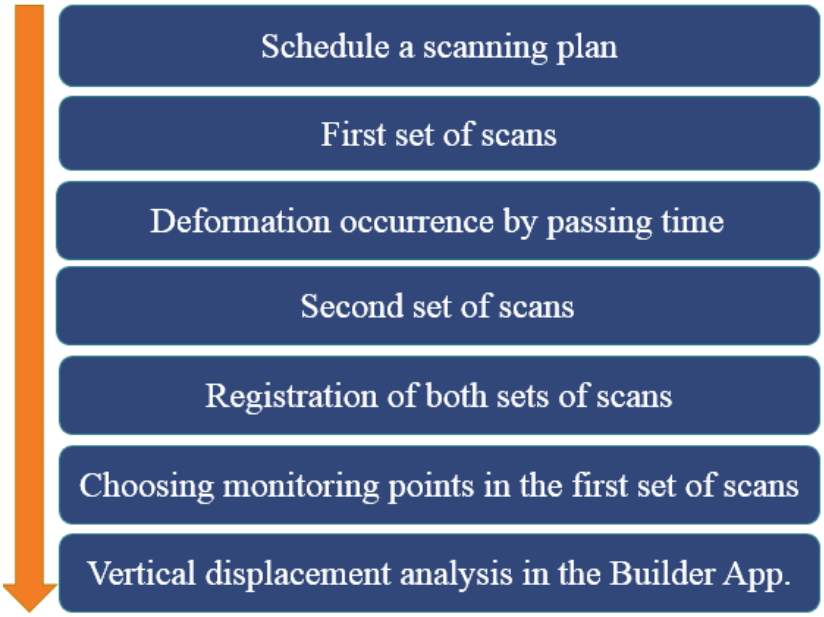

(a)

(b)

(c)

Figure 2. Cutting-edge Technologies (a) Steps for LiDAR Analysis (b) Data Collection using Terrestrial LiDAR (c) Aibotix X6 Hexacopter in Flight

3.3.2 Unmanned Aerial Vehicles (UAV OR UAS)

An unmanned aerial vehicle, also commonly referred to as a drone, is an aircraft that can fly without an actual human pilot on board, and its flight can be controlled from a ground control station (Wen

and Kang, 2014). Rotary wing and fixed wing are the two types of UAV units that are commonly used for commercial purposes. A fixed wing UAV has a single rigid wing across its body that allows it to fly with high speeds and for longer flight distances, similar to manned airplanes (Tahar and Ahmad, 2012). Rotary wing UAV uses lift from the continuous rotation of its blades and has the ability for vertical takeoff and landing, similar to manned helicopters. The main advantages of these systems are that they can access remotely located areas and confined spaces, and can hover at a fixed altitude, allowing sensors (such as digital cameras) to collect precise data from hard to reach areas (Congress et al., 2018).

The Aibot X6 hexacopter, shown in Figure 2b, is designed for a wide range of applications including surveying, infrastructure monitoring, precision agriculture and other areas. Underneath the hexacopter, green LED lights in the front and red LED lights in the back assist in determining its orientation during flight. It has six motor and propeller pairs enclosed in a lightweight composite airframe to handle high winds. It also consists of ultrasonic and barometric sensors that assist in maintaining altitude hold at a safe distance above the ground. The LVP antenna relays the video signals to the digital live video display unit (DLVP). Top and bottom servo gimbals on the copter accommodate and hold different types of sensors. The multi-cable geo-box triggers the camera in accordance with either the flight plan or intervalometer. The X6 has four legs that assist in takeoff and landing operations (Congress, 2018).

The images collected can be geotagged using high quality Real Time Kinematic (RTK) Global Navigation Satellite System (GNSS) data and processed to obtain 3D dense point cloud model, orthomosaics, digital elevation models, digital terrain models, and contours. The navigable 3D models help in a better understanding about the condition of the infrastructure (Anand J Puppala et al., 2018a).

4 LABORATORY INVESTIGATIONS

In order to study the feasibility of remote sensing techniques for identification of pavement distress such as roughness, first, soils are collected from these two sites (US 67 and US 82) and basic soil characterization, strength, stiffness and consolidation property tests are conducted in the laboratory. The behavior of soils after the proposed treatments is assessed in laboratory before the field application.

4.1 Bridge Approach Site

Disturbed soil samples of fill material of the embankment and foundation are collected at the depth of about 3 ft (1 m) depth below the ground and are tested in laboratory to determine the index and engineering properties of the soil samples. The test results of the collected soil samples are presented in Tables 2 and 3 respectively.

Table 2. Physical Properties of the Collected Soil Samples at the Bridge Approach Site

Soil properties	Unit	Embankment fill soil	Foundation soil
Natural moisture content, ω_n	%	18.0	17.2
Dry unit weight	pcf	101.0	112.1
Wet unit weight	pcf	119.2	131.4
Specific gravity of soil solids, G_s	-	2.67	2.70
Percent gravel	%	0.57	0.04
Percent sand	%	61.15	48.67
Percent fine	%	38.28	51.29
Liquid limit, LL	-	32.0	38.0
Plastic limit, PL	-	15.0	17.0
Plasticity index, PI	-	17.0	21.0
Hydraulic conductivity, k	ft./day	0.013	0.0014
Maximum dry density, MDD	pcf	115	114
Optimum moisture content, OMC	%	14.5	14.5
USCS classification	-	SC	CL

Table 3. Engineering Properties of the Collected Soil Samples at the Bridge Approach Site

Soil	Compaction condition	Shear strength		Consolidation			
		c (psf)	ϕ (°)	σ_c' (psf)	e_o	C_c	C_r

Embankment fill soil	Dry of OMC	1,440	30	2,000	0.53	0.26	0.02
	OMC	1,300	26	1,500	0.47	0.27	0.03
	Wet of OMC	1,440	10	2,500	0.54	0.28	0.02
	Natural in-situ	-	-	1,900	0.67	0.30	0.02
Foundation soil	Dry of OMC	-	-	1,800	0.56	0.27	0.02
	OMC	-	-	2,000	0.49	0.28	0.02
	Wet of OMC	-	-	2,100	0.56	0.29	0.02
	Natural in-situ	1,300	12	2,800	0.54	0.30	0.02

4.2 Pavement Heaving Site

The soil samples collected near to the US SH 82 are tested in the laboratory to assess the soil behavior and the effectiveness of the treatments. The test results are provided below.

4.2.1 Swell Strain Test

Swell strains of treated soil specimens collected from the field are determined using the standard procedure as shown in Figure 3b. Figure 4 provides the test results obtained from consolidation apparatus in the laboratory.

(a) (b)

Figure 3. (a) Sample Collection (b) Laboratory Swell Tests

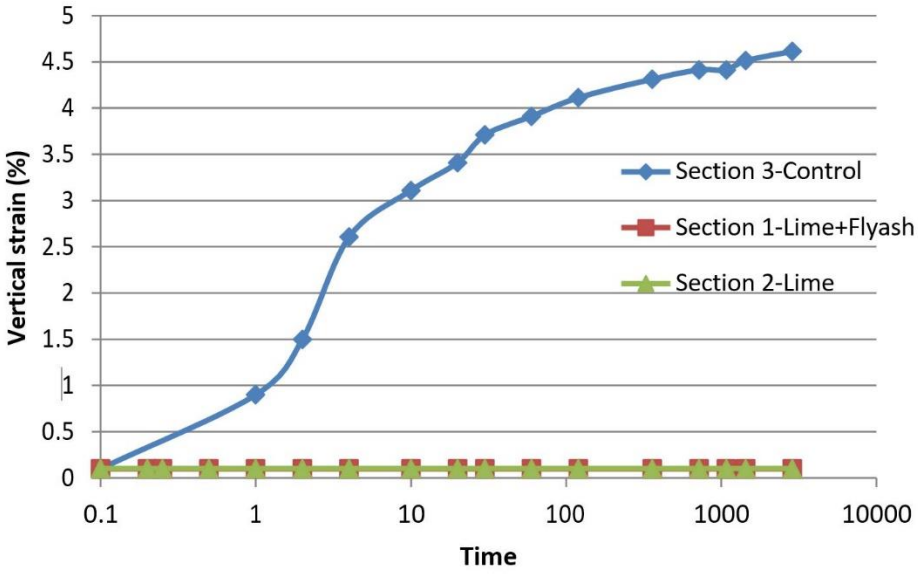

Figure 4. One Dimensional Swell Test Results of Soil Samples Collected during Pavement Reconstruction

It is observed in the above Figure 4, that control soil with lime treatment has shown considerable vertical swell strain of 4.5%, whereas lime (L) + fly ash (FA) treated subgrade with extended mellowing did not show any strains.

4.2.2 Three-Dimensional Free Swell Tests (Volumetric Free Swell Tests)

Three-Dimensional (3-D) free swell test measures the potential of the clay to swell in three (3) directions when soaked under water, as shown in Figure 5. Volumetric strain underwent by the soil specimen is determined by measuring the vertical and radial swell strains. Two identical specimens compacted at their maximum dry density (MDD) and optimum moisture content (OMC) are used for each test section and represented as OMC-1 and OMC-2. Figure 6 presents the vertical swell strain versus elapsed time for the soil samples collected from the test sections. From the test results, it is evident that soil from test section 1 (Lime with FA with extended mellowing) did not exhibit any swelling strain compared to soil samples from test section 3 (control section).

Figure 5. Three Dimensional Swell Test Setup

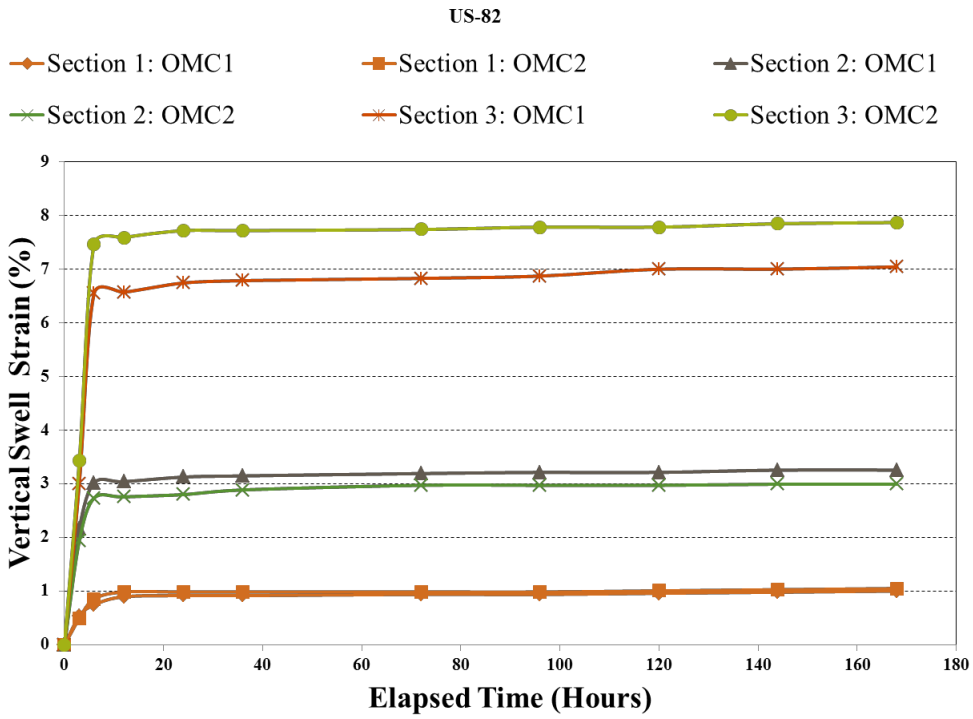

Figure 6. Summary of Vertical Swell Strain Results of Test Sections

Table 4. Vertical, Radial and Volumetric Swell Strains of all test section

Location	Vertical Strain (%)		Radial Strain (%)		Volumetric Strain (%)	
	OMC1	OMC2	OMC1	OMC2	OMC1	OMC2
Section 1	1.15	0.99	0.09	0.19	1.33	1.37
Section 2	3.21	3.05	0.62	0.67	4.45	4.39
Section 3	7.85	7.10	2.99	3.18	13.83	13.46

Table 4 presents the recorded swell strain measurements on samples retrieved from the test site. Three dimensional swell tests conducted at no confinement and complete saturation conditions represent the worst scenario possible to the soil at the field. It is observed that control soil from test section 3 has shown considerable volumetric swell strain of 13.5%, whereas lime + fly ash treated

subgrade with extended mellowing and lime with extended mellowing soils exhibited least swell behavior that represents effectiveness in stabilization procedure.

4.2.3 Reactive Alumina and Silica Assessment Studies

Reactive alumina (Al) and silica (Si) are the aluminum and silica present in amorphous or poorly crystalline Al/Si phases present in the interlayers of montmorillonite. Measuring these concentrations is important since alumina and silica play a predominant role in the formation of ettringite and thaumasite, respectively. Ettringite and thaumasite have been identified as the chief contributors for the heaving of pavements laid over sulfate rich soils (Anand J Puppala et al., 2018b; Talluri et al., 2013). Reactive alumina and silica are measured using Inductively Coupled Plasma-Mass Spectroscopy (ICP-MS) as shown in Figure 7. A modified procedure developed by Foster (1953) is used to determine the amount of reactive alumina and silica. Soil weighing 15gm is mixed with 150mL of 0.5 N NaOH and boiled. After boiling, the solution is centrifuged at 8000 RPM and filtered using a 0.1μm membrane type filter paper. The extract obtained from the filtration process is stored in a plastic bottle to obtain a clear extract that was used for the ICP analysis.

ICP analysis requires a clear solution. The presence of organics or iron oxides in the soils would result in dark colored extract. However, organics can be removed by treating with hydrogen peroxide (H_2O_2) solution. Joffe (1949) reported that the coating of iron oxides (Fe_2O_3) on the clay surface prevent the formation of pozzolanic compounds, as the coating prevents the release of alumina from clay to react with lime. Oxides of iron can be removed by treating 10 ml of the solution with 1 mL of 6N HCl and agitating it every hour. The solution is allowed to settle overnight and 0.1 μm membrane-type filter paper is used to obtain a clear extract, the next morning. After obtaining a clear extract, ICP analysis is performed on the soil samples at varying dilution ratios.

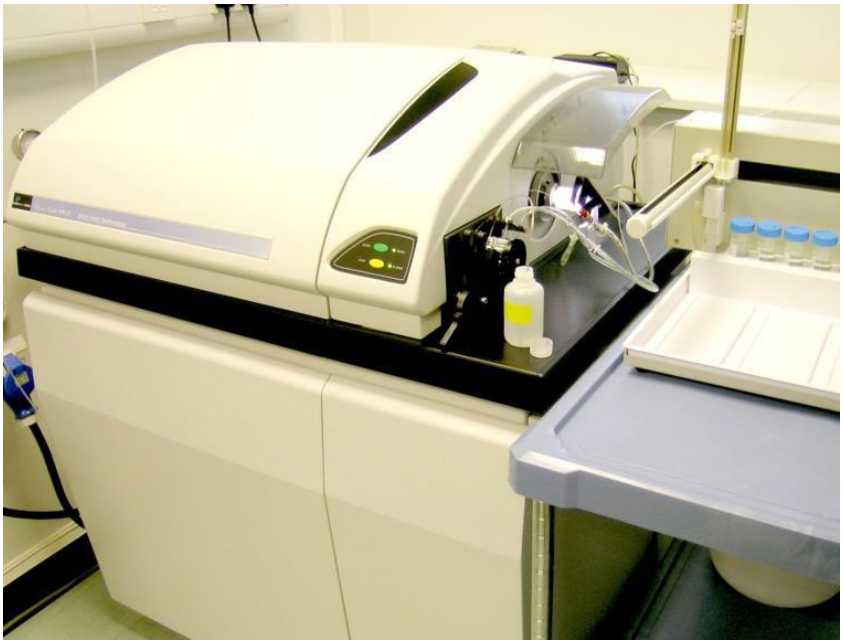

Figure 7. ICP-MS Equipment used for Determination of Silica and Alumina levels

From initial assessment studies prior to construction of US 82, the soils comprise around 323 ppm of reactive alumina (Al) and 187 ppm of reactive silica (Si). During construction/mellowing process the soil is allowed to react with lime and fly ash thereby consuming the available Al and Si in order to accelerate the formation of Ettringite mineral. From recent investigations conducted on April 2015, five core samples are retrieved from US SH 82 pavement section where cracking and heaving is observed. The cores are numbered sequentially beginning at the East End #1 and towards Westbound #5 as shown in Figure 8. Core 1 is within test Section 1 (where lime + FA treatment is conducted), whereas, cores 2, 3, 4 and 5 are collected from pavement with conventional lime with 3 day mellowing construction. Table 5 presents the reactive alumina and silica measurements obtained from the core samples retrieved.

Figure 8. Core samples retrieved from US 82 Pavement Site

Table 5 summarized reactive alumina (Al) and silica (Si) levels of the samples retreieved from five coring sites along US 82 pavement section. All locations have lower reactive Al levels compared to initial reading of 323 ppm prior to construction. Similarly, silica levels at locations C3, C4 and C5 decreased from their initial reading of 187 ppm. This shows that portion of the available Al and Si might have been consumed towards the formation of Ettringite prior to construction. However, at locations C1 and C2, reactive Si levels increased to 269 ppm and 226 ppm, respectively. This could be attributed to the addition of fly ash during the stabilization process near test section 1.

Table 5. Reactive Alumina and Silica Measurements

Location	Reactive Al (ppm)		Reactive Si (ppm)	
	Mean	St. Dev	Mean	St. Dev
C1	174.8	0.6	169.1	5.3
C2	143.8	0.3	126.2	0.8
C3	47.6	0.2	113.4	1.4
C4	118.3	0.3	158.7	1.2
C5	227.3	1.2	68.6	0.3

5 FIELD STUDIES

5.1 Bridge Approach Site

A 40-ft high bridge situated on US 67 over SH 174 in Johnson County, Cleburne, Texas has undergone more than 17 in. of settlement since its construction in 1995. Figure 9 presents the location of the bridge. Several rehabilitation measures such as soil nailing, hot mix overlays, foam slab jacking, and compaction grouting were attempted to mitigate this settlement thus alleviating the bump problem at the end of the approach slab. However, none of the rehabilitation techniques were effective. In 2012, Texas Department of Transportation, Fort Worth district (TxDOT-FTW) installed the light weight EPS geofoam as an embankment fill material to mitigate the bump phenomenon. The current research is performed to effectively collect the elevation profiled data of the bridge approach embankment using remote sensing data methods.

Figure 9. US 67 Bridge Approach Embankment Test Site

5.1.1 LiDAR Survey *Data Collection and Analysis*

To evaluate the geofoam embankment performance, LiDAR surveys are performed at the test site to measure the displacements over a wider area encompassing the bridge deck, approach slabs, pavement shoulders, and embankment slopes. These were performed using a FARO 3D laser scanner in different time periods. Figure 2 presents the steps for performing the LiDAR surveys and analysis. After several test trials at the US 67 test site, an optimized LiDAR survey comprising

of 10 different scan locations are determined, as shown in Figure 10. Small anchors to which spheres can be fixed, as shown in Figure 11, are installed at the US 67 bridge infrastructure to serve as ground control points required for the analysis.

Figure 10. Scanning locations and top view of the monitored Area

Figure 11. Installed anchors and reference spheres

The first LiDAR survey was performed in April 2016 and the elevations determined from this analysis is used as the reference for measuring deformations for later surveys. To monitor vertical movements at the top of the pavement, two grids of points are chosen over grid dimensions of 98' x 32' as shown in Figure 12. The red dots indicate the monitoring points on the approach slab, whereas the blue dots represent the monitoring points on the bridge deck.

Figure 12. Set of Monitoring Points Placed over the Bridge Approach and the Deck

It is observed that the monitoring points at the top of the bridge approach embankment (red color dots) have different altitudes in comparison to the monitoring points located at the top of the bridge deck (blue color dots). Several other monitoring points are also selected at the pavement shoulder to assess the side slope embankment movements (see Figure 13).

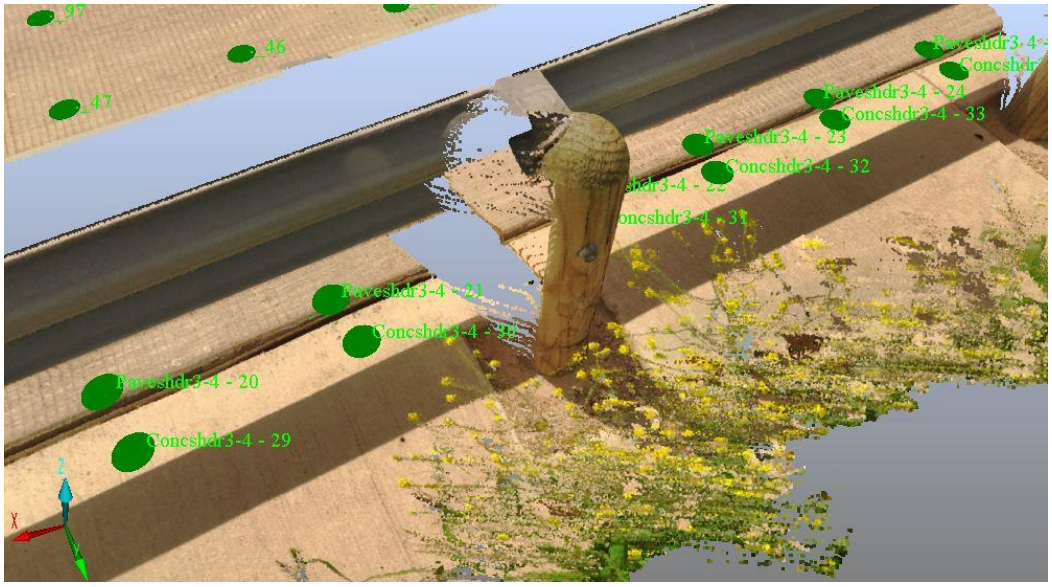

Figure 13. Monitoring Points on the Side Slope and Pavement Shoulder

The analysis performed on the monitoring points on the bridge deck from LiDAR surveys is conducted from the collected between April 2016 to May 2016 and showed negligible vertical movements. However, vertical deformation analysis on the bridge approach embankment revealed

that heaving had occurred at the bridge approach embankment (Figure 14). It should be noted that the negative values in Figure 14 represent heaving and positive values indicate settlement.

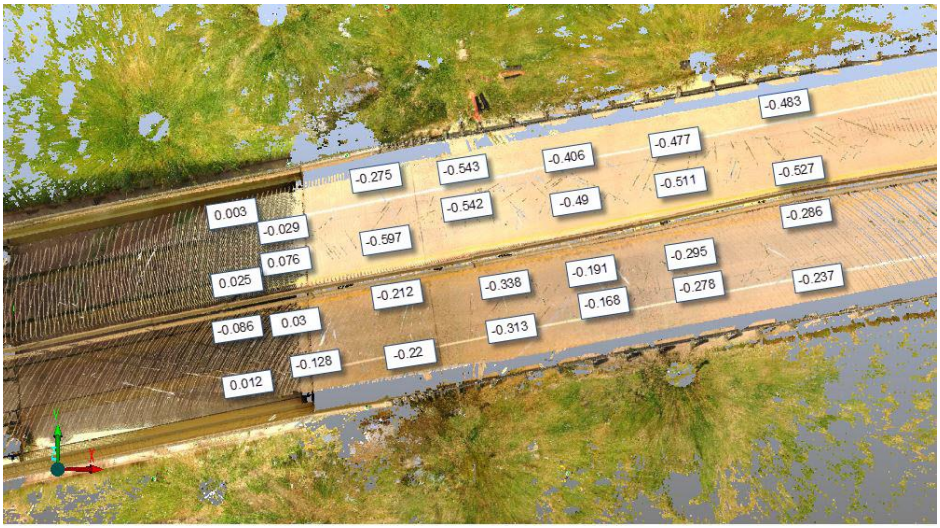

Figure 14. Vertical Deformations from April 2016 to May 2016 (from LiDAR surveys)

Similarly, analysis is performed on the scan data obtained in the month of July 2016. Figure 15 depicts cumulative total vertical deformations at the top of the pavement from April 2016 to July 2016. It is evident from the figure that one lane had undergone heaving and the other lane had experienced settling.

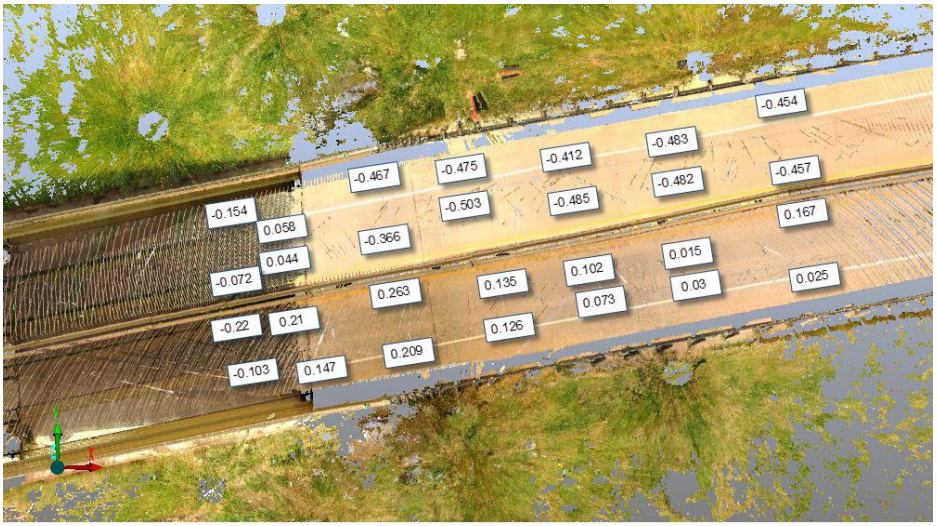

Figure 15. Cumulative total vertical deformations from April 2016 to July 2016

Comparison studies are performed for the deformations determined from LiDAR analysis and inclinometer data analysis. It is observed that both monitoring methods provided similar trend

patterns and settlements were within the tolerance limits. However, the LiDAR surveys provided vertical displacement information over the wider area. Hence, it can be concluded that the performance of the geofoam at this test site is satisfactory as the settlements subsided and are well within threshold levels.

5.2 Pavement Heaving Site

The pavement laid over problematic soils was rehabilitated by stabilization methods and this research study identified the need for quickly identifying any trace of heaving caused due to the presence of high sulfates. The objective of this data collection is to monitor the 300 ft (91 m) long and 23 ft (7 m) wide pavement stretch for identifying the undulations on the surface profile that indicate the presence of heaving, shown in Figure 16. The US state highway 82 data obtained from remote sensing techniques involving terrestrial LiDAR and Unmanned Aerial Vehicle (UAV) are analyzed to assess the condition of the pavement laid over problematic soils.

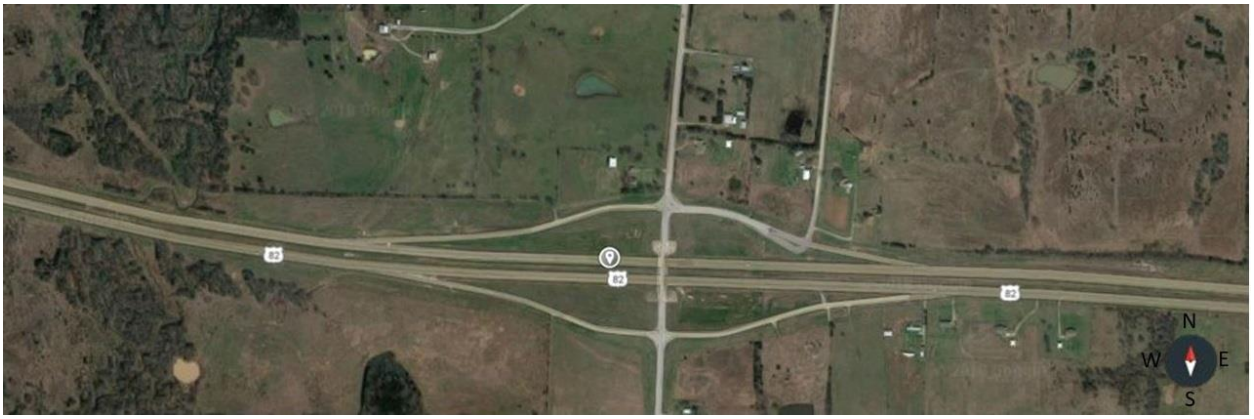

Figure 16. US 82 Pavement Heaving Test Site

5.2.1 LiDAR Studies

LiDAR studies are performed using a FARO 3D laser scanner. Data is stitched and analyzed using SCENE software. The stitched data is used to obtain the cross slope of the pavement. Cross slope can be defined as the rate of change in the height of the pavement in the transverse direction. In the event of rain, cross-slope of the pavement is important to ensure that there is ample drainage. The ultimate goal is that there is no ponding or stagnant water on or near the pavement; this will prevent hydroplaning from impeding the available skid resistance. It also prevents moisture intrusion into underlying expansive subgrades and thereby mitigates differential movements of

pavement. At turns, it is also necessary to check if there is sufficient transverse slope i.e. super elevation providing necessary centripetal force for a safe turn.

In total five LiDAR scans are conducted to obtain the data of the pavement stretch under inspection. One of the LiDAR scan locations can be observed in the top right corner of the Figure 17. The pavement cross slope is obtained from the elevation difference and the distance between the two points selected on the boundaries of the two lane pavement as shown below. The length of the line selected over the pavement is 293.30 in. and the elevation difference of the two points was 9.42 in. The transverse slope of 3.2% obtained from the LiDAR data.

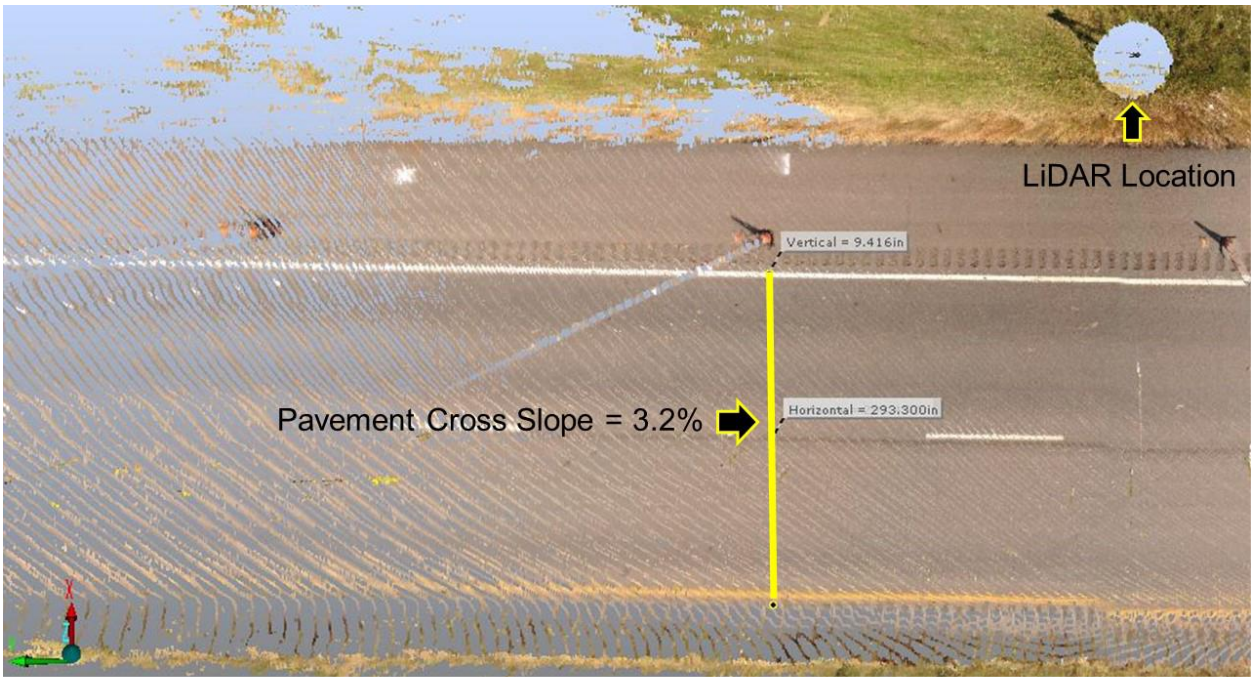

Figure 17. Transverse Slope Computed from LiDAR Data

5.2.2 Unmanned Aerial Vehicles (UAV)

Cautionary signs are placed on both directions of the highway during the aerial data collection studies conducted at the site. No traffic regulations, except the placing of cones on the shoulder of the pavement, are imposed while collecting the data from the drone flying away from the pavement. Both the longitudinal and transverse slopes of the pavement are calculated from the same pavement data collected at multiple flight altitudes at 20 ft and 75 ft, respectively. The UAV is flown at a safe distance of 10 ft away from the pavement section. Hence, the camera angle is

inclined towards the pavement while flying at 20 ft high and in the nadir position while flying at 75 ft high; this is to ensure full transverse coverage of the pavement site.

Due to the vegetation on the pavement shoulder, a large wooden plank is placed to serve for landing and take-off. The images are processed to obtain 3D dense point cloud model, orthomosaics, digital elevation models, digital terrain models, and contours of the inspected pavement area. Before analyzing the pavement data for heaving problem, the quality of the imagery data is checked by comparing the data accuracy with LiDAR.

Due to the availability of dense point cloud models, the cross slope of the pavement is calculated at desired longitudinal spacing on the pavement section. For better representation, the cross slope is computed with points placed in the transverse direction of the pavement at 0.4 inch (1 cm) intervals. Transverse direction is selected according to AASHTO PP 70-10, which defines a transverse line as a line that deviates less than 10° to the perpendicular line of the pavement centerline. The transverse slope is calculated at 30 ft intervals along the longitudinal direction of the pavement. The cross slope sections provided in Figure 18 show a slope of 3.2% sloping towards the shoulder (indicated by the green colored arrows in the top and profile views). This can also be observed in the profile section view provided where the white and yellow pavement markings and the centerline of two lanes can be seen at the bottom of Figure 18.

It shows that the shoulder of the pavement, over which the traffic cones are placed, was at a lower altitude compared to the other side of the pavement in the transverse direction. The cross slope values obtained from LiDAR and UAV analysis has shown good match, indicating the accuracy of the aerial data.

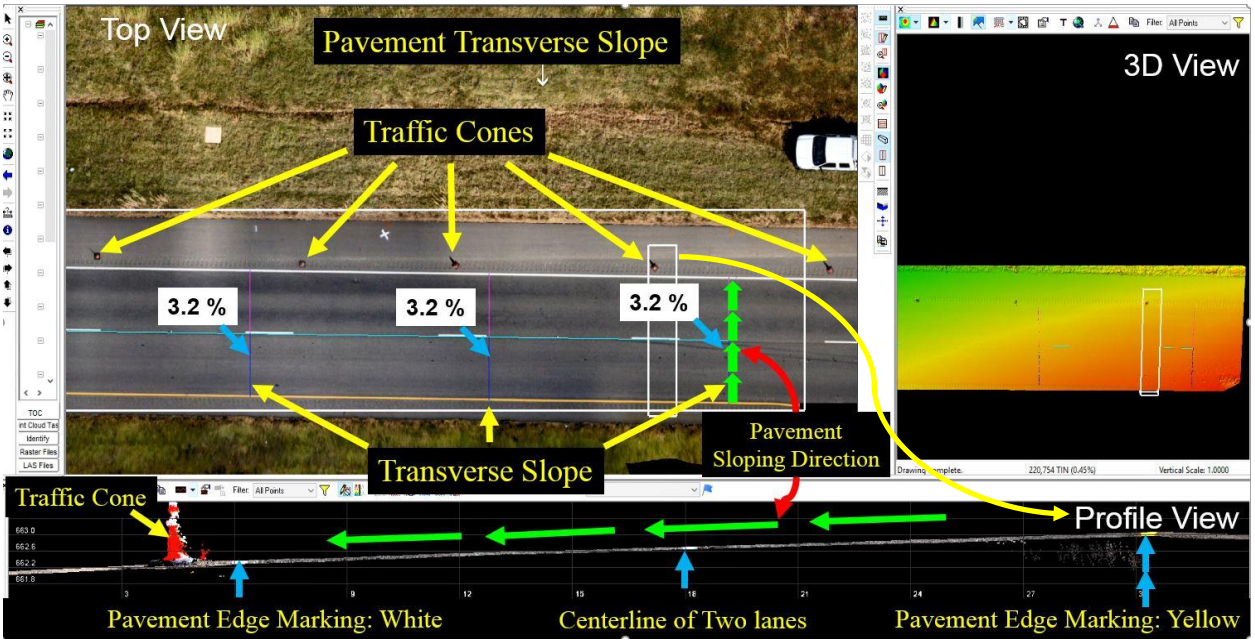

Figure 18. Transverse Slope Computed Along Three Paths

The processed models from UAV data are then analyzed for various pavement distress and characteristics. Due to the earlier reported heaving problem prior to the treatment of problematic sulfate soils underneath the pavement, the elevation profile of the treated is estimated to spot undulations. The estimated longitudinal elevation profile is also helpful in estimating the International Roughness Index (IRI) that indicates the comfort of the road passenger. Pavement wheel paths are defined basing on AASHTO PP 69-16 and AASHTO PP 70-10 standards. The longitudinal elevation profiles shown in Figure 19 have indicated that there is no heaving that has occurred after treating the soils with high sulfates.

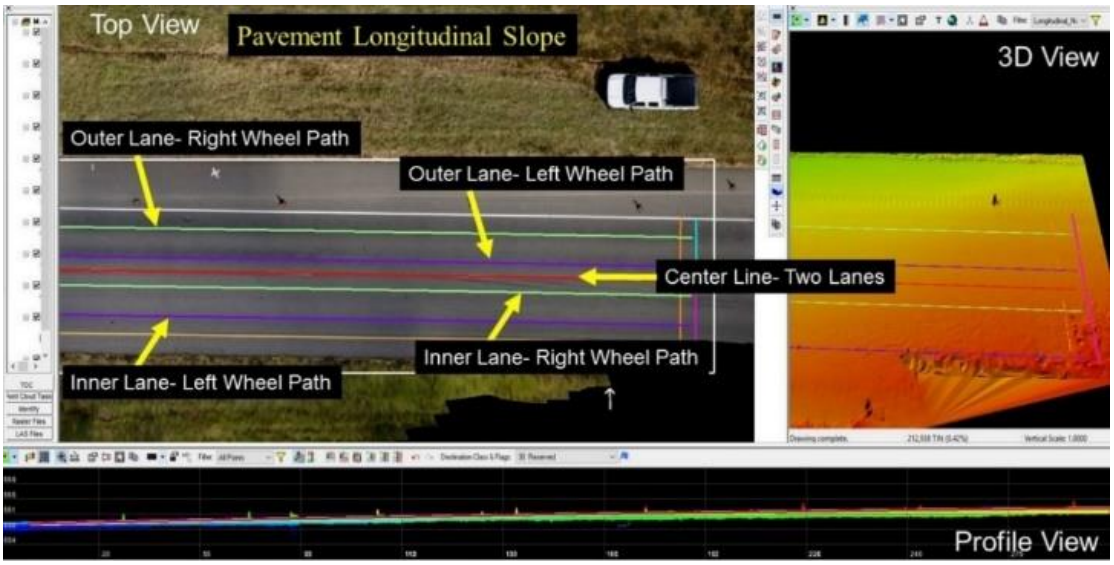

Figure 19. Pavement Longitudinal Slope along the Two Wheel Paths of Each Lane and Data Points at 1-cm Interval along 300 ft Stretch

Due to the enormity of the elevation data comprising of more than 10,000 points for each wheel path, elevation profiles of four wheel paths within a 100 ft (30 m) section along the vehicular direction of pavement are compiled, and these results are provided in Figure 20. Elevation profiles of outer lane right wheel path represented by orange; outer lane left wheel path represented by red; inner lane right wheel path represented by dark blue; inner lane left wheel path represented by cyan, are shown in Figure 20. The horizontal distance between the starting point of the 100 ft (30 m) stretch and all points within the stretch are plotted along X-axis and their corresponding elevation differences with the starting point are plotted on Y-axis.

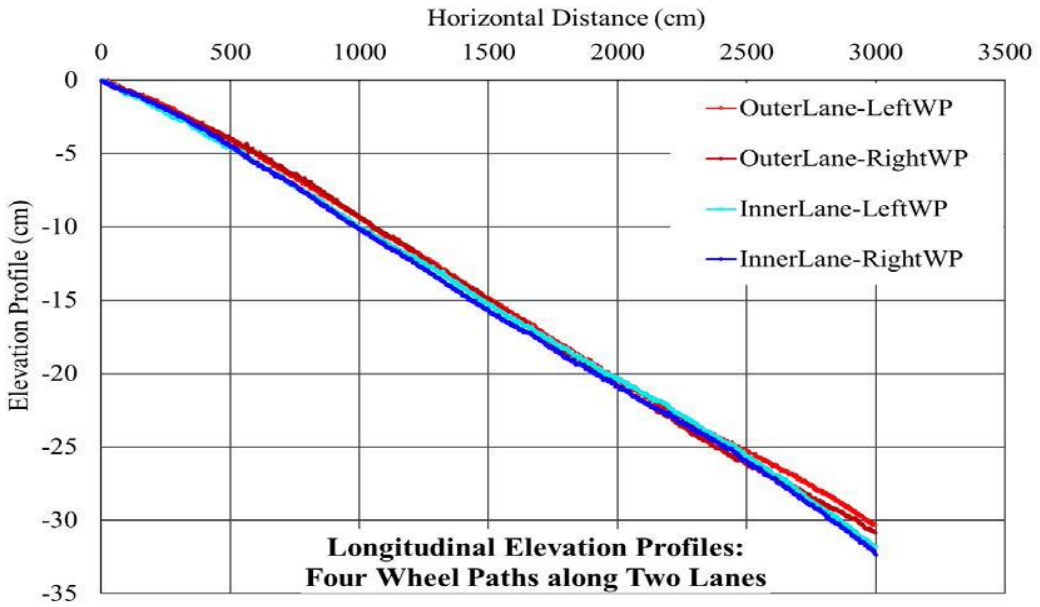

Figure 20**.** Longitudinal Elevation Profiles of Four Wheel Paths along Two lanes of the Pavement

Analysis of the pavement characteristics data collected from UAV-CRP methodology proved efficient and accurate. This methodology helped in transforming the present subjective inspections to objective by providing repeatable and reproducible data.

6 SUMMARY AND CONCLUSIONS

Remote capturing of the pavement data as discussed in this research has been effective in collecting the health data that helps in assessing the condition of the infrastructure. Some of the conclusions on this approach are provided below.

- LiDAR analysis performed on the bridge infrastructure have shown that there are only negligible vertical movements. Vertical deformations that occurred at the approach embankment indicated the presence of heaving and shrinking. However, those magnitudes are within the allowable limits.
- Vertical deformations obtained from inclinometers and LiDAR surveys resulted in similar vertical trends. However, the LiDAR surveys offer a dense point cloud and provided the deformations over a wider area.
- LiDAR studies have concluded that using EPS geofoam blocks as a lightweight

embankment fill material is effective in controlling the differential settlements of an embankment thereby preventing the formation of the bump at the end of the bridge.

- The dense point cloud data obtained from terrestrial LiDAR and UAV have shown good correlation, hence it is proposed to be used as a complimentary data collection tool to the traditional methods.
- The longitudinal elevation profile of the US SH 82 pavement laid over high sulfate soils collected from UAV has indicated that there are no abrupt changes in elevations. This validates the effectiveness of extended mellowing period treatments in arresting the heaving.
- Due to the emerging nature of UAV technology, it can be used as a complimentary data collection tool to the present traditional methods.

7 ACKNOWLEDGMENTS

The authors gratefully acknowledge the support and generosity of the Center for Transportation Equity, Decisions and Dollars (CTEDD), for its partial support towards this work. The authors would like to express their sincere appreciation to the TxDOT. The authors would also like to acknowledge the University of Texas Arlington team members Cody Lundberg, Ujwalkumar Patil, Tejo Vikash Bheemasetti, Arvanid Pedarla, Pinit Ruttanaporamakul, Nagasreenivaasu Talluri Ali Shafikhani, and He Shi for their help during data collection.

8 REFERENCES

Alavi, S., LeCates, J.F., Tavares, M.P., 2008. Falling weight deflectometer usage.

Alshibli, K.A., Abu-Farsakh, M., Seyman, E., 2005. Laboratory evaluation of the geogauge and light falling weight deflectometer as construction control tools. J. Mater. Civ. Eng. 17 5 , 560–569.

Congress, S.S.C., 2018. Novel Infrastructure Monitoring Using Multifaceted Unmanned Aerial Vehicle Systems - Close Range Photogrammetry (UAV - CRP) Data Analysis. University of Texas at Arlington, Arlington, Texas.

Congress, S.S.C., Puppala, A.J., Lundberg, C.L., 2018. Total system error analysis of UAV-CRP technology for monitoring transportation infrastructure assets. Eng. Geol. 247. doi:10.1016/j.enggeo.2018.11.002

Foster, M.D., 1953. Geochemical studies of clay minerals III. The determination of free silica and free alumina in montmorillonites. Geochim. Cosmochim. Acta 3 2–3 , 143–154.

Joffe, J.S., 1949. The ABC of soils. Oxford Book Company.

Puppala, A.J., Asce, F., Ruttanaporamakul, P., Tejo, ;, Bheemasetti, V., Asce, A.M., Shafikhani, A., 2018. Laboratory and Field Investigations on Geofoam. doi:10.1061/(ASCE)PS.1949-1204.0000364

Puppala, A.J., Congress, S.S.C., Bheemasetti, T. V, Caballero, S.R., 2018a. Visualization of Civil Infrastructure Emphasizing Geomaterial Characterization and Performance. J. Mater. Civ. Eng. 30 10 , 4018236.

Puppala, A.J., Intharasombat, N., Vempati, R.K., 2005. Experimental studies on ettringite-induced heaving in soils. J. Geotech. Geoenvironmental Eng. 131 3 , 325–337.

Puppala, A.J., Talluri, N., Congress, S.S.C., Gaily, A., 2018b. Ettringite induced heaving in stabilized high sulfate soils. Innov. Infrastruct. Solut. 3 1 , 72. doi:10.1007/s41062-018-0179-7

Puppala, A.J., Talluri, N.S., Chittoori, B.S., Gaily, A., 2012. Lessons learned from sulfate induced heaving studies in chemically treated soils, in: Proceedings of the International Conference on Ground Improvement and Ground Control. Research Publishing. pp. 85–98.

Ruttanaporamakul, P., 2015. Evaluation Of Lightweight Geofoam For Mitigating Bridge Approach Slab Settlements.

Tahar, K.N., Ahmad, A., 2012. A simulation study on the capabilities of rotor wing unmanned aerial vehicle in aerial terrain mapping. Int. J. Phys. Sci. 7 8 , 1300–1306.

Talluri, N., Puppala, A., Chittoori, B., Gaily, A., Harris, P., 2013. Stabilization of high-sulfate soils by extended mellowing. Transp. Res. Rec. J. Transp. Res. Board 2363 , 96–104.

Wen, M.-C., Kang, S.-C., 2014. Augmented reality and unmanned aerial vehicle assist in construction management, in: Computing in Civil and Building Engineering (2014). pp. 1570–1577.

CENTER FOR TRANSPORTATION EQUITY, DECISIONS & DOLLARS

The **Center for Transportation, Equity, Decisions and Dollars (CTEDD)** is a USDOT University Transportation Center, leading **transportation policy research** that aids in **decision making** and **improves economic development** through **more efficient, and cost-effective use of existing transportation systems,** and offers **better access to jobs and opportunities.** We are leading a larger consortium of universities focused on **providing outreach** and **research to policy makers**, through **innovative methods** and **educating future leaders of the transportation field.**

UNIVERSITY OF TEXAS ARLINGTON

CAL POLY SAN LUIS OBISPO

Georgia Tech

USF UNIVERSITY OF SOUTH FLORIDA

WISCONSIN UNIVERSITY OF WISCONSIN–MADISON

C-TEDD@UTA.EDU | CTEDD.UTA.EDU | @UTACTEDD | @ C__TEDD | @ CENTER FOR TRANSPORTATION, EQUITY, DECISIONS AND DOLLARS | 817.272.5138